Corrosion Science 202 (2022) 110311

Contents lists available at ScienceDirect

Corrosion Science

journal homepage: www.elsevier.com/locate/corsci

A new insight into the rate determining step of cathodic delamination

N. Khayatan [a,*], M. Rohwerder [a]

[a] Max-Planck-Institut für Eisenforschung GmbH, Max-Planck-Straße 1, 40237 Düsseldorf, Germany

ARTICLE INFO

Keywords:
Organic coatings
Scanning Kelvin Probe (SKP)
Polarisation
Cathodic delamination
Rate determining step
Oxygen reduction

ABSTRACT

One of the most important mechanisms of organic coating degradation is cathodic delamination. Although a significant progress towards the fundamentals of delamination was achieved in the recent decades, the underlying key parameters are not fully understood. It is believed that either cation migration along the delaminated interface or oxygen reduction at the interface are rate determining. However, as will be shown here this is not the case. A new hypothesis, which is cation insertion into the intact interface as the rate determining step in delamination, is proposed using a combined Scanning Kelvin Probe/potentiostat set-up and an in-depth delamination rate analysis.

1. Introduction

Organic coatings are widely used to protect metals against corrosion and to provide aesthetic properties and other functionalities such as thermal insulation, friction, signal colors, electrical insulation. Degradation of the coatings can occur due to various mechanical, thermal, chemical, and biological conditions. Degradation by electrochemical reactions underneath the coatings is a common cause of organic coatings failure, which might take place in mechanisms such as blistering, anodic undermining, filiform corrosion and cathodic delamination [1,2]. The latter is one of the most important degradation mechanisms, which mostly takes place on steel and zinc substrates. Cathodic delamination, which is initiated and driven by corrosion at a defect site in the coating or at the interface, is a laterally proceeding loss of adhesion between organic coating and metallic substrate. This phenomenon has attracted the attention of many scientists for decades. One of the first studies on the delamination mechanism was carried out by Leidheiser et al. in 1983 [3]. Later in the 1990s, a significant breakthrough was achieved by Stratmann et al., who applied Scanning Kelvin Probe (SKP) in corrosion science. Kelvin Probe, a non-contact and non-destructive method, was adopted for investigation on atmospheric corrosion of metals and polymer coated metals, where conventional electrochemical techniques are not applicable [4–12].

A detailed delamination model of polymer coated steel using SKP as the main technique was first presented by Leng et al. [13–15]. In brief, upon activation of corrosion by adding the electrolyte into the defect, the electrode potential of the defect shifts negatively towards the free corrosion potential of iron, which is determined by anodic metal dissolution (Eq. (1)) and the oxygen reduction reaction (ORR) (Eq. (2)) in the defect:

$$Fe \longrightarrow Fe^{2+} + 2e^{-} \quad (1)$$

$$O_2 + 2H_2O + 4e^{-} \longrightarrow 4OH^{-} \quad (2)$$

Typical potential profiles as they are characteristic for delamination of polymer coated steel/iron are schematically shown in Fig. 1. The dissolution of iron is inhibited on the intact coating/iron interface due to the absence of electrolyte, which results in a potential in the passive potential range, i.e. relatively high, with a high ratio of $[Fe^{3+}]/[Fe^{2+}]$ in the oxide film, which inhibits oxygen reduction [16] as well as the relatively large upward band bending [17]. The potential difference between the defect and the intact interface is a driving force for cation migration [18]. A galvanic coupling is formed between the defect and the adjacent interface by incorporation of cations into the interface. This causes a negative shift of the potential at the interface, which enables the onset of oxygen reduction at the buried interface by lowering or even lifting the upward band bending and increasing the Fe^{2+} concentration at the surface of the passive layer.

The intermediate radicals formed during ORR attack the bonds between the organic coating and the metal as well as the organic matrix at the interface and thus delamination occurs [13]. The sharp potential transitions that can be seen in the potential profiles shown in Fig. 1 mark the delamination front, which moves away from the defect. The galvanic coupling between the net local anode (defect) and the net local cathode (delamination front) results in an ohmic potential drop along the delaminated interface, which increases as the front goes further.

* Corresponding author.

https://doi.org/10.1016/j.corsci.2022.110311
Received 18 February 2022; Received in revised form 7 April 2022; Accepted 9 April 2022
Available online 13 April 2022

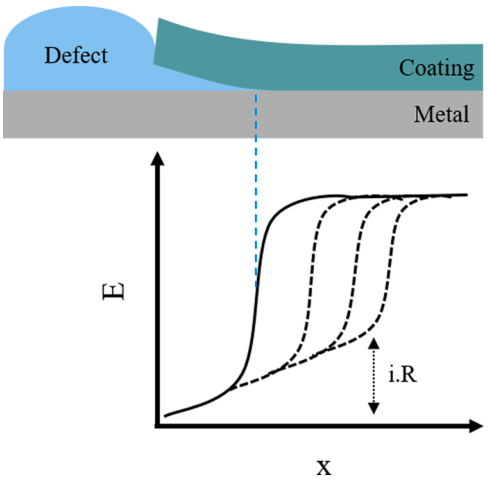

Fig. 1. A schematic illustration of delaminating interface and the respective potential profile. The potential drop across the delamination front is decreasing by ohmic i.R drop in the delaminated interface.

As the delamination front is discernible by SKP, the progress of delamination with time can be monitored, which makes it possible to calculate the delamination rate. It is stated in the literature [14,19] that delamination progress with time follows the power function (Eq. (3)):

$$x\,(t) = k(t - t_i)^a \tag{3}$$

where x is the delamination front position, k the rate constant, t the delamination time, t_i the initiation time, and a the exponent, usually varying from 0.5 to 1. It is generally agreed that the delamination progress that depends on square root of time ($a = 0.5$) is controlled by the cation migration from the corroding defect to the delamination front, while a linear progress with time ($a = 1$) is attributed to the oxygen reduction reaction as rate determining step [14,19–33]. Usually, it is found that faster delaminating "weaker" coatings show a rather square root of time dependence, while slower delaminating "stronger" coatings show a constant delamination rate. However, this is not of general validity. For instance, Nazarov et al. reported of quite strong coatings showing a square root of time dependence [30].

It has been shown that the delamination of simple non-pigmented coating from steel [14] and electrogalvanized steel [19] seem to be controlled by cation migration along the delaminated interface, which consequently results in slower progress for bigger hydrated cations in the electrolyte. However, it was found that presence of more than 1 vol % of CO_2 in the atmosphere significantly decreases the delamination rate on electrogalvanized steel, which was proposed to be due to the change of delamination mechanism to a charge transfer control, resulting in a linear progress with time.

This seems to be supported by observations where inhibition of oxygen reduction seems to lead to a change from a parabolic rate to a linear rate of the delamination progress. For instance, the effect of polyaniline additions to PVB coating on the delamination of the resulting composite coating on iron was investigated by Holness et al. [24]. A transition from parabolic (for simple PVB) to linear delamination kinetics (for polyaniline dispersed PVB) was shown. The authors attributed this to the reduced activation-controlled rate of ORR, which was replaced to some extent by polyaniline reduction at the delamination front, releasing paratoluenesulfonic anions, which unlike ORR products, do not destroy the coating/metal bonds. This leads to a quite significant decrease of delamination rate. In more recent work by Merz et al. [34,35], it is proposed that this effect, in fact, is due to the polarization of the interface surrounding the polyaniline particles, which prevents the potential to be pulled down in the first place.

In another study by Glover et al. [29], the delamination kinetics of PVB coating containing graphene nano-platelets (GNP) from iron and zinc was investigated. It was shown that the delamination rates remained parabolic in case of zinc substrate, but they changed to linear for iron substrate. The latter was linked to the longer path of oxygen permeation through the coating in presence of GNP in the coating. For zinc substrate, however, the presence of GNP was proposed to increase the required charge for unit area of delamination, which would lead to higher required cation migration. It was also mentioned that GNP pigments act as an oxygen cathode on zinc, which results in more dissolution of zinc underneath the coating, leading to a more gelatinous delaminated interface and to a reduced cation mobility.

However, the best fit for the exponent a in Eq. 3 is often neither quite 0.5 nor 1. Furthermore, it seems counter-intuitive that the delamination rate of a coating should be determined by cation migration along the delaminated interface, which would mean that the nature of the intact interface plays no role. This indicates that there is great scope for further studies. The aim of the present work was to fundamentally investigate the role of key parameters in cathodic delamination mechanism and to improve our understanding of the delamination kinetics, which could take our knowledge one step forward. A novel, combined Scanning Kelvin Probe/potentiostat set-up was used to evaluate the generally accepted theories and to propose a new hypothesis about rate determining step in cathodic delamination.

2. Experimental

2.1. Materials

Iron (99.8%) sheet with a thickness of about 1 mm was used as substrate for the samples. Potassium chloride (KCl, p.a.), lithium chloride (LiCl, p.a.), polyvinyl butyral (PVB), agar, pure ethanol, platinum wire (99.99%- diam. 1.0 mm) were purchased from Sigma-Aldrich. Potassium oxalate monohydrate ($K_2C_2O_4{\cdot}H_2O$, 98.5–101.0%), lithium oxalate ($Li_2C_2O_4$, 99 +%), and silver wire (99.99%- diam. 0.25 mm) were purchased from Alfa Aesar. Copper sulphate ($CuSO_4$, 99.7%) was supplied by VWR. A two-component cold curing glue (X60) was purchased from HBM. Microscope slides (0.8–1.0 mm) were purchased from Thermo Scientific. The aqueous solutions were prepared by ultra-pure water using USF ELGA system with a conductivity less than 0.055 μS/cm. PVB solution (10 wt%) was prepared using pure ethanol.

2.2. Sample preparation

Iron sheet was cut into 30 × 20 mm^2 pieces, which then were ground with sequentially finer silicon carbide sandpapers of up to P1000. The pieces were rinsed with ultra-pure water and cleaned in an ultrasonic bath for 5 min in pure ethanol, then were dried using high pressure air stream. PVB solution was applied on the iron substrates using a spin coater at 2000 rpm for 20 s two times with 30 s waiting in between. Then the coating was cured in an oven at 75 °C for 10 min. In order to prepare samples with a corroding defect, an iron plate with the same dimension and preparation was stuck underneath the coated iron along the sample by cold curing glue, providing free iron in front of the coated iron (see Fig. 2a). The electrical connection between the iron plates was

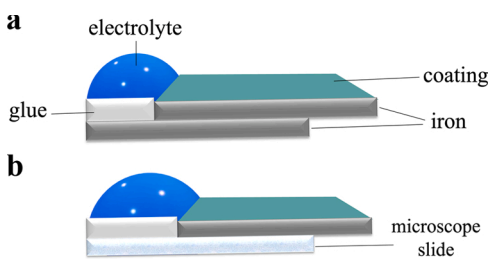

Fig. 2. A schematic drawing of the sample prepared for a) corrosion driven experiments b) potential-controlled experiments.

provided by copper tape. For potential-controlled defects, a piece of microscope slide was stuck underneath the coated iron by glue (see Fig. 2b), providing an electric insulation setting for placing the electrodes.

2.3. SKP measurements

For the monitoring of coating delamination and cation migration a commercial Scanning Kelvin Probe (SKP) from KM Soft Control was used, which was operated with a Ni(80)/Cr(20) tip (~100 μm in diameter) [36]. The resolution of the SKP measurements is linked to the tip diameter and the step size of scanning. The step size was set to either 10 or 20 μm for all the measurements and the tip diameter was about 100 μm, which should provide a lateral resolution of better than 100 μm. The potential is measured with an accuracy better than 1 mV, but slight drifts of potential are observed, which can be controlled by regular re-calibration on the $Cu/CuSO_4$ reference. The relative humidity in the chamber was maintained between 91% and 94%. Prior to any measurement, the SKP tip was calibrated against a $Cu/CuSO_4$ (saturated solution) reference electrode in air at R.H.~93%. All the potentials are reported versus the Standard Hydrogen Electrode (SHE). The starting point of the measurements was about 1000 μm away from the artificial defect in all experiments. The line scans were done at the middle of the width along the length of the samples. A MATLAB program, developed by Schulz [37], was used to process the SKP data.

2.4. Combined SKP/Potentiostat set-up

In order to apply any potential of interest at the defect site during SKP measurements, a combined SKP/potentiostat set-up was built, which is schematically shown in Fig. 3. A portable compactstat from IVIUM technologies was used as potentiostat. A micro Ag/AgCl [38] and a Pt wire were used as reference and counter electrodes in a 3-electrode set-up, with the iron edge exposed at the defect as working electrode (Cu tape was used to electrically connect the Fe sample on the microscope slide to the stage). All the other conditions were identical to the free-corroding defect experiments, explained in the previous part (2.3). To prevent strong anodic corrosion at high potentials in the defect, aqueous oxalate solutions were used as electrolyte instead of aqueous chloride solutions with the same molarity of cations. The experiments including free corrosion driven and potential-controlled experiments were replicated at least 4 times in each condition (i.e. for each different kind of electrolyte).

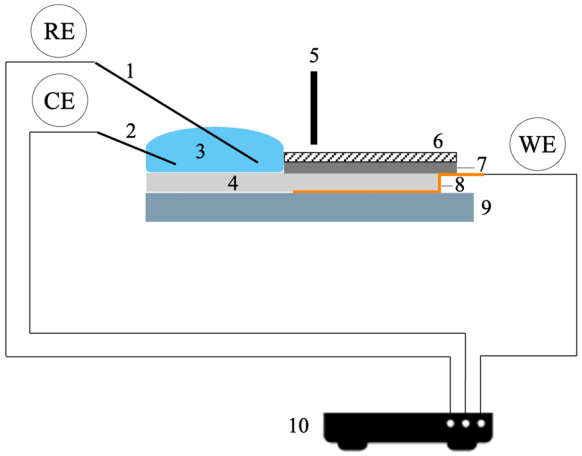

Fig. 3. A schematic illustration of the combined SKP/potentiostat set-up used for potential-controlled experiments, 1: Ag/AgCl micro-reference electrode, 2: Pt wire as counter electrode, 3: electrolyte, 4: microscope slide, 5: SKP tip, 6: coating, 7: metal, 8: Cu tape, 9: SKP stage, 10: potentiostat.

3. Results and discussion

In order to investigate whether the rate determining step in cathodic delamination is indeed the cation migration from the defect to the delamination front as is assumed according to the generally accepted theory, a potential-controlled experiment was designed using the combined SKP/potentiostat set-up. Fig. 4 shows the potential profiles obtained by SKP on PVB coated iron, already delaminated about 4500 μm, with an aqueous solution of 0.5 M $K_2C_2O_4$ in the defect, which was polarized to different potentials while SKP was scanning the surface. The first curve (black line) was obtained by polarizing the defect to − 0.65 V vs. SHE, which shows a high ohmic drop in the delaminated interface. The second curve (blue line) was obtained by starting with the same polarization in the defect but changing the potential in the defect to − 0.25 V vs. SHE at around x = 2000 μm while SKP was scanning the surface. It can be clearly seen that the potential at the distance of 2000 μm away from the defect rose immediately by changing the potential in the defect, which indicates cation migration along the delaminated interface takes negligible time, and therefore, it is unlikely to be rate determining in cathodic delamination. The third curve (red line) was obtained by starting with the applied potential of − 0.25 V in the defect and going back to − 0.65 V at x = 2000 μm while SKP was measuring the potential of the interface. As can be seen, the potential in 2000 μm distance from the defect decreased immediately to the values when − 0.65 V was applied in the defect from the beginning (the first curve/black line). Note that the potentials in the delaminated interface of a passive metal are always higher than the potentials in the defect, due to the ohmic i.R drop along the delaminated area. These results fundamentally show that cation migration in the delaminated interface is fast, and therefore, unlikely to control the delamination kinetics.

In order to have reference measurements for an in-depth analysis, first standard delamination experiments on PVB coated iron with free-corroding defects were performed. Fig. 5a-b shows the delamination curves for 1 M KCl and 1 M LiCl in the defects, respectively. The corresponding progress of delamination is shown in Fig. 5c, which for both cases indicates an initial dependence of the delamination progress on the square root of time (see Fig. 5d)). In accordance with the findings reported by Leng et al. [14], the delamination for the case of Li^+ as cation in the defect was slower than that with K^+, which is proposed to be due to the larger size of the lithium cation due to the more pronounced hydration shell. This, at first glance, suggests that cation migration from the defect is the rate determining step in these delamination experiments, just like it was proposed in these earlier works; however, it should be noted that there is an ohmic potential drop in the delaminated interface, which could also play a role in affecting the delamination

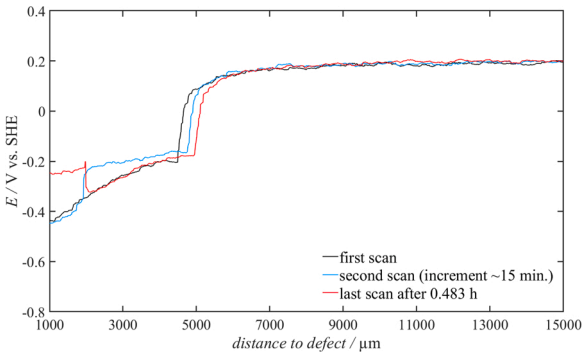

Fig. 4. Delamination curves as obtained by SKP on a PVB coated iron sample with an aqueous solution of 0.5 M $K_2C_2O_4$ in the defect, which was polarized to − 0.65 V vs. SHE (black line). The potential was changed from − 0.65 V to − 0.25 V vs. SHE at around 2000 μm distance to the defect (blue line), followed by a change back to − 0.65 V vs SHE in the next scan at the same position (red line). As can be seen the response in potential at the delaminated interface is nearly immediate. Scan rate: 1.17 mm/min.

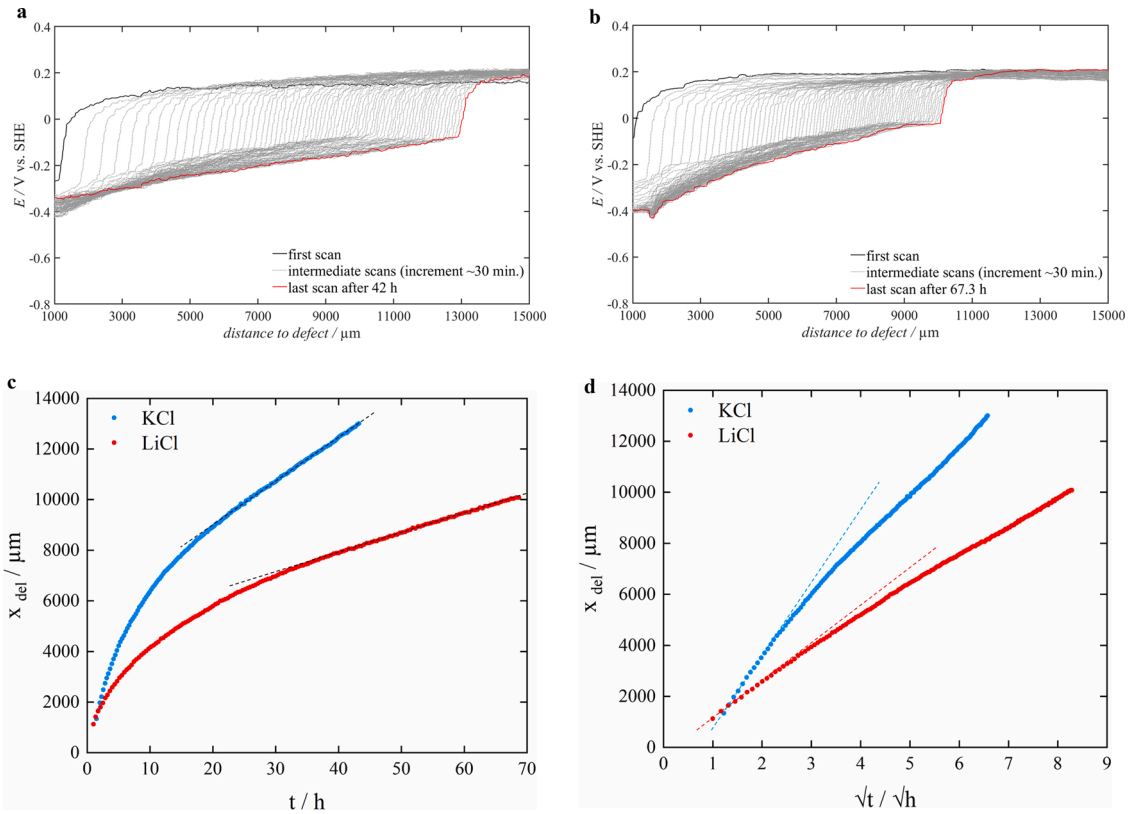

Fig. 5. Delamination curves as obtained by SKP on PVB coated iron samples with an aqueous solution of a) 1 M KCl, b) 1 M LiCl in the defect, c) the delamination progress with time, and d) as a function of square root of time. In (c) the later linear behavior and in (d) the initial sqrt(t) behavior are indicated by dashed lines.

rates. It should be noted that with progress of the delamination, the ohmic i.R drop at the delaminated interface leads to a steady increase of the potential at the delamination front. This in turn should decrease the driving force for delamination, which is widely assumed to be the potential difference between delaminated interface and intact interface at the front. An inversion of this difference fully inhibits delamination [17]. Therefore, the obtained delamination behavior, i.e. the initial square root of time dependence that can be seen in Fig. 5d, could have been influenced by the decreased driving force, and is not necessarily attributed to the cation migration from the defect. This point is frequently neglected in the delamination rate analyses.

In order to understand the effect of ohmic potential drop along the delaminated interface on the delamination rate, potential-controlled experiments were performed on PVB coated iron for two different electrolytes in the defects. Fig. 6a-b shows the delamination curves obtained by subsequently increasing the potential applied in the defect for the case of either 0.5 M $K_2C_2O_4$ (a) or 0.5 M $Li_2C_2O_4$ (b) as electrolyte. As especially for the higher potentials oxygen reduction and hence delamination will be quite inhibited, it is anticipated that at higher potentials the progress of the steep change in potential in the potential profiles is not indicating the delamination front but rather the front of migrating cations along the intact interface, just like cations are just migrating along the intact interface in argon atmosphere [15]. Hence, in the following we denote this progressing front as the delamination/migration front. The progress of the delamination/migration front versus time is shown in Fig. 6c-d, which were derived from (a) and (b), respectively. It can be seen that the progress is inclined to a linear dependence on time by increasing the potential in the defect, and subsequently, removing the ohmic drop in the delaminated interface. This effect can be seen more clearly in Fig. 7, where there is only a high potential applied over extended time. At such a high potential, it is not expected to have much oxygen reduction, therefore, as mentioned the progress of the front has to be related to the cations, moving along the interface. Yet, the rates in Fig. 7c show a linear dependence on time, and not a parabolic one that is expected in ionic migration. Hence, the result could not be explained by cation migration, which parabolically depends on the distance to the defect. In fact, the cation migration that is accordance with the potential profiles of Fig. 7 are unlikely to show a parabolic behavior. The reason why diffusion and migration often show a square root of time dependence is that the gradient of concentration or potential gets shallower and shallower upon advance of diffusion or migration. As can be seen, there is no sign of such characteristic smear-out of potential over time. On the contrary, there is always a steep potential change at the front, and only a very small potential drop, if any, in the migrated area. Hence, it seems that the transport of cations towards the front cannot be the rate limiting step here. It rather looks like that the rate determining step is not along the migrated interface, but rather at the migration front.

In order to elucidate this further, an in-depth rate analysis was carried out on the delamination/migration curves shown in Figs. 5 and 6. In Fig. 8 the logarithm of the rates obtained from these curves is plotted as a function of the according potentials at the front. The range of data is limited to the natural corrosion potential of delamination in case of free corrosion driven experiments (potassium and lithium chloride in the defect). As can be seen, the rates are the same at same potential and cation in the defect, regardless of whether oxalate or chloride was used in the defect., i.e. whether free corrosion or polarization by potentiostat determined the potential in the defect. As can also be seen in Fig. 8, the rates are different for the same potential at the front, but different size of the cation, i.e., K^+ and Li^+. This is another proof for excluding oxygen reduction reaction as the rate determining step, since oxygen should not much depend on the cation in the double layer region (at least not for such similar ones). On the other hand, it was just shown that cation migration from the defect site cannot be the rate determining step as well (see Fig. 7). These findings and analyses have led us to propose a new hypothesis about the rate determining step in delamination, which

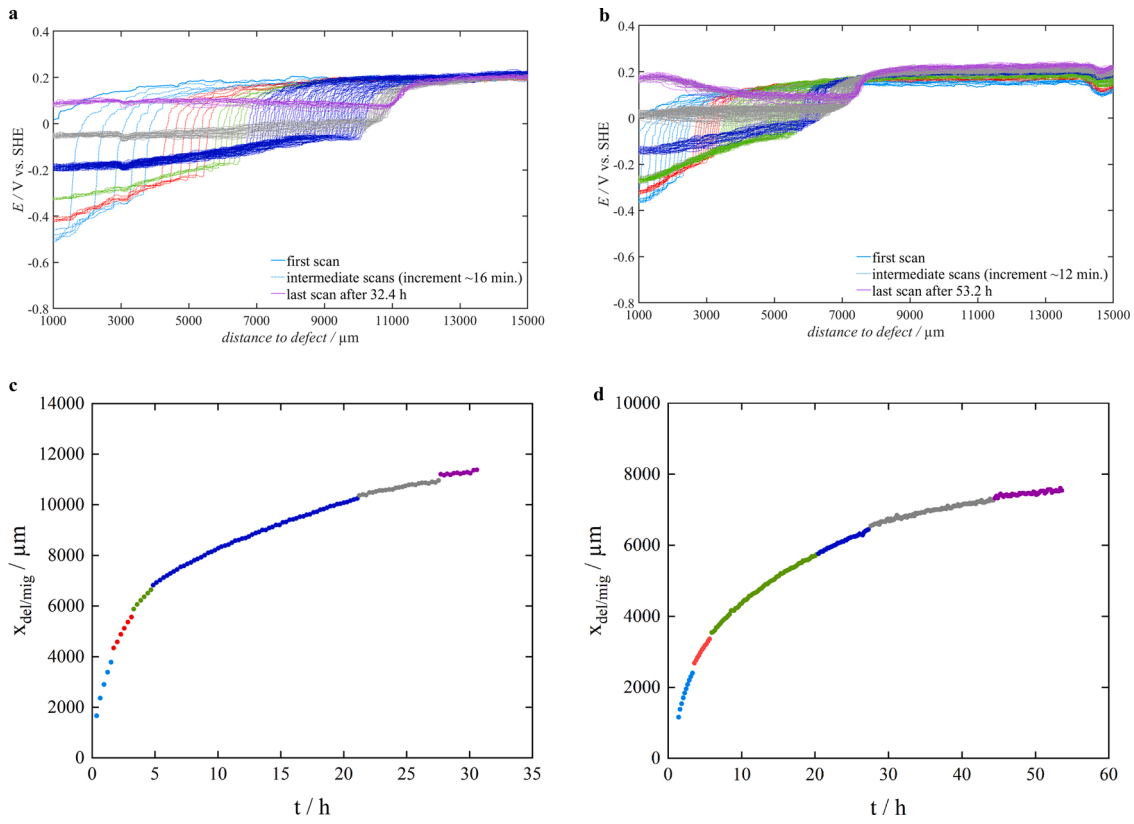

Fig. 6. a,b) Delamination curves as obtained by SKP on PVB coated iron samples with an aqueous solution of a) 0.5 M $K_2C_2O_4$ b) 0.5 M $Li_2C_2O_4$ in the defect, which were polarized to subsequently increasing potentials. Each color marks the delamination curves obtained at a certain applied potential. c,d) progress of the delamination/migration front as a function of time, which were derived from (a) and (b), respectively. Same color as used in (a) and (b) shows the progress at the same applied potential.

will be elaborated in the following.

Thus far, the role of cations in cathodic delamination has been solely discussed as migration of cations from the corroding defect to the intact interface, i.e., along the delaminated interface. This cation migration is required in order to ensure charge neutrality, i.e., to compensate the electron flow along the interface from the defect to the delaminating and delaminated interface, which is required for the oxygen reduction reaction at the pulled down potentials. Without this migration, the potential could not stay such low. It was assumed that a square root dependence on time for the overall delamination rate is associated with cation migration as the rate determining step [14]. However, the results obtained in this work cannot be explained by this generally accepted theory. We here propose that the first insertion of cations into the cation-free intact interface is the rate determining step in delamination, which is schematically shown in Fig. 9. This hypothesis correlates the delamination rate with the resistance of the bonds and pore structure at the intact coating/metal interface, instead of assuming that the already delaminated interface controls the kinetics. Furthermore, it agrees well with the obtained data, i.e., it simultaneously considers the role of cations, and explains the progress of the front that linearly changes with time at constant potential at the front (see Fig. 7), i.e. in absence of an iR drop at the migrated interface. Other indications for this hypothesis were also discovered in earlier research. It was found that adsorbed species such as CO_2 on coated zinc [39] and even O_2 on novel chromium coatings [33] have a huge effect on delamination/migration. Since the delaminated interface is characterized by relatively high rates of oxygen reduction during delamination and for the case of zinc also by anodic zinc oxidation and dissolution, it seems unlikely that the presence of e.g. small amounts of CO_2 could have a significant effect on ion mobility at that interface. This means that the observed effects are most likely related to the intact interface, i.e., the initial cation insertion step into the intact interface.

Through this new hypothesis, it is now easier to explain the behavior in Fig. 8. The linear dependence of the logarithm of the rates on potential seems to be split in two regions: a low potential region and a high potential region. In the latter the slope of the linear dependence is higher than in the low potential region. This could be linked to a higher driving force for cation insertion at the front in case of delamination at the front (low potential region), due to the according significant increase in the cation concentration in the delaminated interface. Hence, it would mean that the behavior in the low potential range is characterized by delamination almost directly following the steep front in the potential profiles, while the behavior at high potential rather corresponds to a migration process without delamination, or delamination slowly following the front. This can also be seen in the evolution of the curves upon the potential switch between grey and violet curves in Fig. 6a-b. In the left part of the “delaminated” region, close to the defect, where low potentials were applied in the previous steps, the potentials are fully pulled up towards the now applied high potential in the defect, whereas in the right part of the “delaminated” region, where only high potentials were applied, the potentials are not fully pulled-up, which means that only migration occurred there.

However, it is difficult to explain why the rate of insertion of cations at the front is a function of electrode potential just at the bottom of the steep front. Intuitively, one would rather see the potential drop across the front as a driving force for insertion. In fact, the mere presence of such a steep front indicates that the key processes occur here. As already pointed out above, if mere migration from the defect to the front was rate determining, then no steep front would be expected, but rather a gradually increasing potential, extending from the defect to the front. As the slope becomes gentler with increasing distance between defect and front, the rate gets slower, causing the typical sqrt(t) behavior. This is

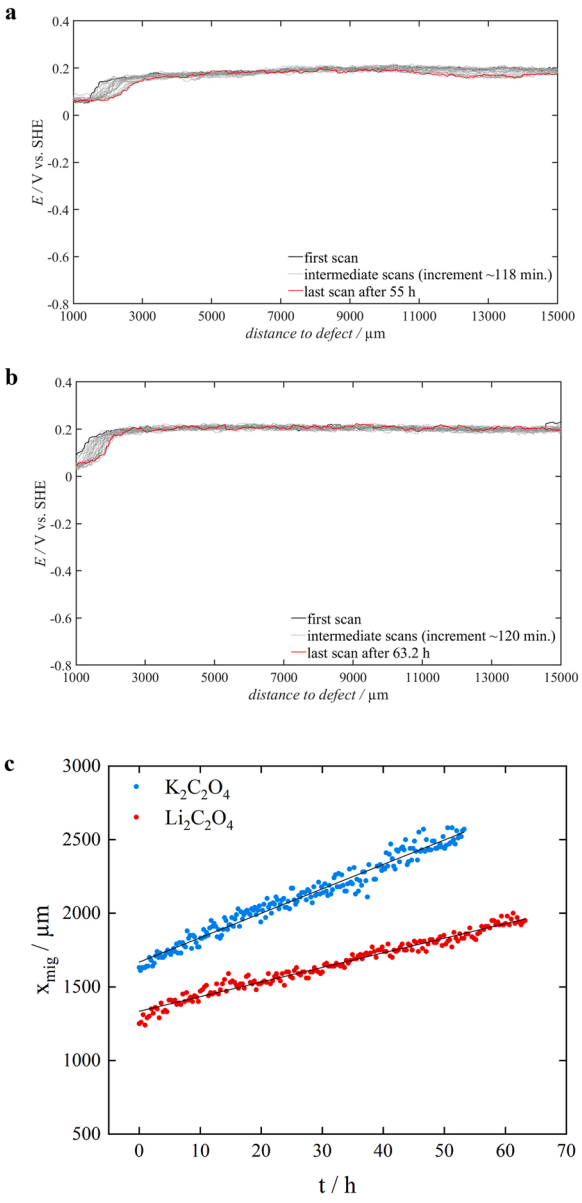

Fig. 7. a,b) Migration/insertion curves as obtained by SKP on PVB coated iron samples with an aqueous solution of a) 0.5 M $K_2C_2O_4$ in the defect which was polarized to + 0.050 V vs. SHE b) 0.5 M $Li_2C_2O_4$ at the same potential in the defect, both measured after pre-exposure, c) the corresponding rates.

not the case here. Concerning the driving force for cation insertion at the steep front, it seems obvious that this should be the electric field at the front. This could in principle be obtained from the potential curves recorded by SKP. However, since the resolution of SKP is limited and the front moves during the measurement, the front is known to be smeared out in the recorded curves, especially for fast progress at lower potentials. Hence, the slopes at the front obtainable from the experimental results are subject to significant artefacts. For this reason, it was decided to take the potential difference between the intact interface potential and the potential just at the bottom of the steep potential front as a first approximation of the driving force. Fig. 10 shows the delamination/migration rate in a logarithmic scale as a function of this potential drop across the front.

Figs. 8 and 10 also depict the data derived from standard (corrosion driven) delamination of PVB coated iron with 1 M KCl and 1 M LiCl in the defect, which have the same cation concentration as 0.5 M oxalate solutions used in potential controlled experiments. In these standard

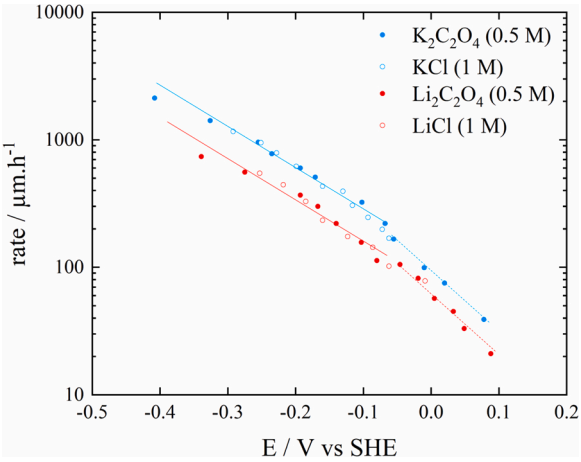

Fig. 8. Dependence of delamination/migration rate on potential at the beginning of the steep front for PVB coated iron samples with 0.5 M $K_2C_2O_4$, 0.5 M $Li_2C_2O_4$, 1 M KCL and 1 M LiCl as electrolyte in the defect, which were derived from Figs. 5 and 6. For this the delamination curves were analyzed in small sections, where the potential at the front was assumed to be roughly constant and the according local rate was determined.

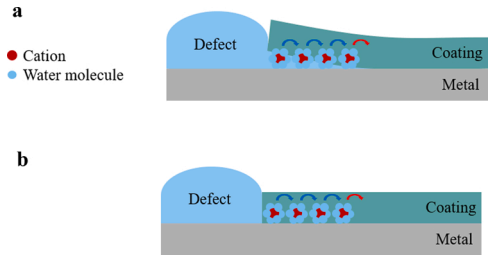

Fig. 9. Schematic illustrations of migration of cations a) along the delaminated interface and b) along the intact coating/metal interface. The blue arrows indicate movement of cations along the interface into which cations already have migrated, the red arrow shows the next step of the cation at the front, where it has to jump into the yet unaffected interface, which is denoted here as cation insertion into the intact interface.

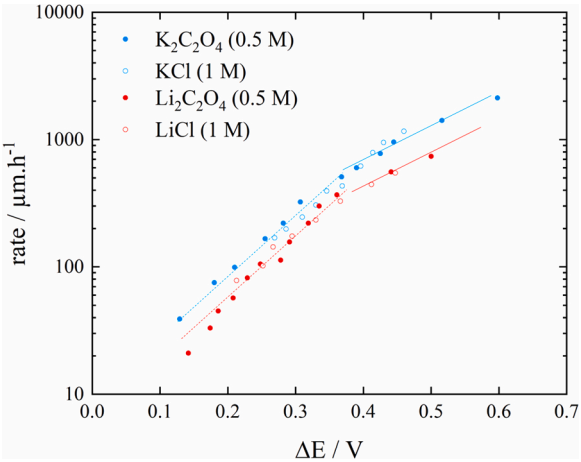

Fig. 10. Dependence of delamination/migration rate on potential difference across the delamination front for PVB coated iron samples with 0.5 M $K_2C_2O_4$, 0.5 M $Li_2C_2O_4$, 1 M KCL and 1 M LiCl as electrolyte in the defect, which were derived from Figs. 5 and 6.

experiments, the potentials at the front (or the potential drop across the front) are changing due to iR drop in the delaminated interface, which leads to a steady decrease of the driving force. For potentiostatically controlled potential a wider range of potentials could be covered. Here the driving force was reduced stepwise by increasing the applied potential stepwise to higher values. As mentioned above, the data obtained for the same cation in the different electrolytes fits well with each other, indicating anions do not play a role in cathodic delamination, in agreement with prior work [14].

The higher rate for K^+ compared to Li^+ is supporting the idea that the rate determining step is correlated to ionic mobility, since small Li^+ cation, due to its higher charge density, has a bulkier hydration shell and is hence less mobile [40]. As discussed above, the lower or higher rate is not due to the slower or faster cation migration from the defect to the front, since migration is not the rate determining step here. In fact, it is due to the insertion of cations into the yet intact (and cation-free) coating/metal interface, which is the rate determining step, and will obviously be affected by the cation size, i.e., the bigger the hydrated cations, the slower the insertion.

In order to study the hypothesis about cation insertion in more detail, delamination experiments were conducted on PVB coated iron with low concentrations of 0.05 M and 0.01 M KCl solution in the defect. The corresponding delamination curves obtained by SKP are shown in Fig. 11a-b. For comparison, the delamination curves of 1 M KCl solution in the defect (Fig. 5a) is added and shown in Fig. 11c (note that there are offsets in the time scale, due to the different pre-exposure times of the samples). The free corrosion potential in the defects was comparable in all cases (~ −0.5 V vs. SHE). Nevertheless, only 1 M electrolyte pulled down the potential of the affected interface to low values characteristic for delamination. This could be explained by considering the two distinct driving forces for cation movements: potential gradient, and ion concentration gradient.

At the border between the defect and the coating/metal interface, the electrochemical potential of a cation such as K^+ is as follows:

$$\widetilde{\mu}_{k,el} = \mu_{k,el} + z_k F\varphi_{el} = \mu^0_{k,el} + RTlnx_{k,el} + z_k F\varphi_{el} \quad (4)$$

and similarly, the electrochemical potential of a cation at the interface is:

$$\widetilde{\mu}_{k,int} = \mu_{k,int} + z_k F\varphi_{int} = \mu^0_{k,int} + RTlnx_{k,int} + z_k F\varphi_{int} \quad (5)$$

where $\widetilde{\mu}$ is the electrochemical potential, μ the chemical potential, μ^0 the standard chemical potential of the cations, z electron valence, F Faraday's constant, x cation concentration, and φ Galvani potential. Since the standard chemical potential of the cations in the intact interface is considerably higher than in the electrolyte, a driving force is needed so that cations enter the interface. As mentioned, there are two driving forces, the difference in concentration and in potential: the concentration in the defect filled with electrolyte is significantly higher than that at the interface (initially the concentration is zero at the interface) and the Galvani potential is notably lower at the interface than in the electrolyte in the defect (note that although the electrode potential is higher

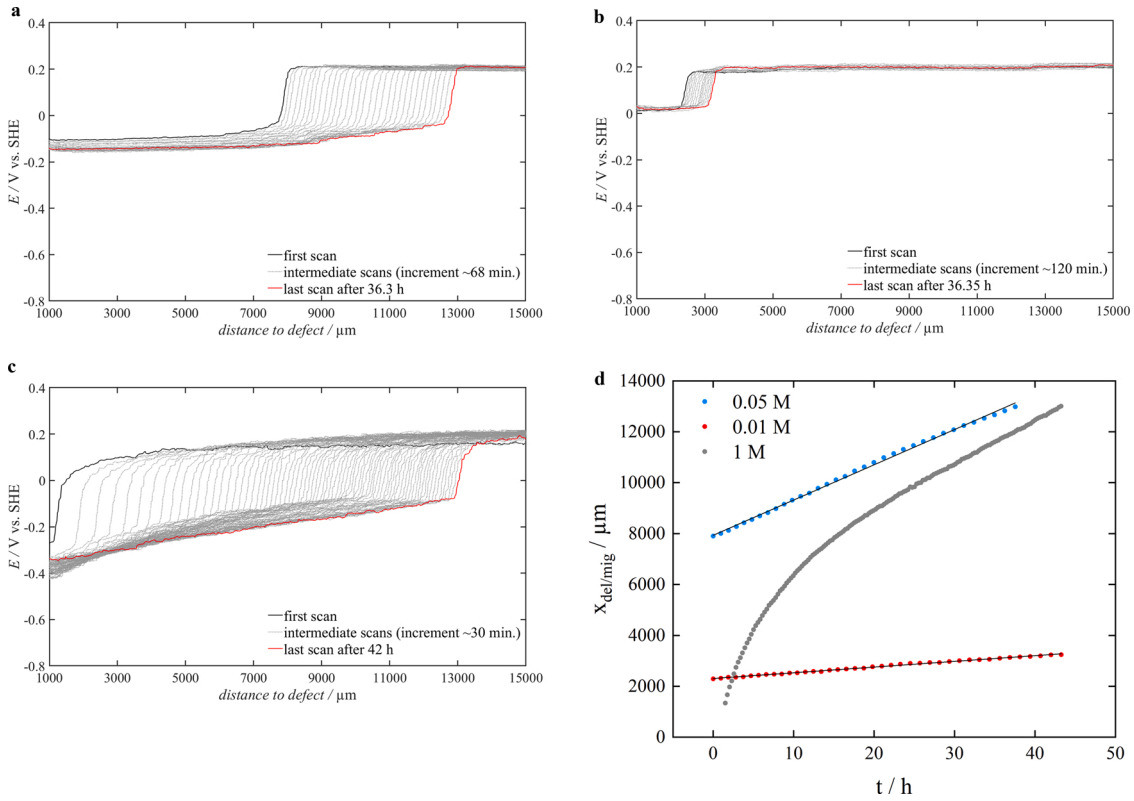

Fig. 11. Potential profiles as obtained by SKP on PVB coated iron samples with an aqueous solution of a) 0.05 M, b) 0.01 M, and c) 1 M KCl in the defect. The corrosion potential in the defects was comparable in all three cases (~ −0.5 V). As can be seen, with decreasing concentration of potassium cations in the defect the ingress and migration of cations at the interface results in decreasingly pulled-down potentials due to the lower number of potassium cations entering the interface. For 0.05 M and 0.01 M KCl the potentials established at the interface are much higher than the potential in the defect, indicating no delamination occurred in these cases. This is due to the potentials at the interface, which are obviously too high to lead to enough oxygen reduction reaction required for delamination (ORR). Hence, since no ORR needs to be supported by additional cation flow along the interface, no Ohmic drop along the interface is observed. The progress of the front as a function of time is depicted in (d), which shows linear progress with time, i.e. at a constant rate, for 0.05 M and 0.01 M KCl in the defect (note that the samples with 0.05 M and 0.01 M KCl was started ex-situ, i.e. already delaminated for a while before these measurements were made), and non-linear progress with time for 1 M KCl in the defect. In the latter case, the potential was pulled down towards the defect potential. At these lower potentials, oxygen reduction occurs and a visible Ohmic iR drop is established.

at the interface, the Galvani potential is lower in the phase above the metal, since the Galvani potential in the metal is the same at the defect and the interface, see e.g. [18] and Fig. 12).

Hence, both concentration and potential in the defect can serve as driving force for the ingress of cations into the interface. It should be noted that the interfacial properties are most probably changed as a consequence of hydrated ion incorporation at the interface, and therefore, $\mu^0_{k,int}$ might not be constant along the interface, changing from more ion containing interface to still intact interface without any migrated ions. This will be especially the case if due to the pulled down electrode potential, caused by the cations moving into the interface, the interface starts to degrade as a consequence of onset of ORR. However, this can be neglected at the early stage discussed here.

Fig. 11 shows that for lower concentrations of electrolyte a lower pulling down of potential (lower pulling up of φ_{int}) occurs compared to that in the high concentration of electrolyte (1 M KCl, Fig. 11c), which means that a lower amount of cations ingresses into the interface. The amount is determined by the equilibrium defined by Eqs. (4) and (5). This also indicates that obviously no delamination occurs in the case of low concentrations of 0.01 and 0.05 M KCl in the defect, as otherwise the potential would be further pulled down towards the potential of the defect. Delamination does not occur in these cases, because at the related high potentials at the interface oxygen reduction is still quite inhibited, whereas for the high concentration of 1 M KCl, delamination occurs and the potential at the interface is pulled towards the defect potential. This is due to the degradation by ORR, and subsequently, the effective Galvanic coupling established by delamination. The high ORR rates also cause a high Ohmic iR drop along the delaminated interface. It is highly interesting that the progress of the delamination/migration front is linear with time for the low concentrations of electrolyte (see Fig. 11d), while for the high concentration it shows a sqrt(t) dependence, which in accordance with the hypothesis proposed here is caused by the according decrease of potential difference across the delamination front, i.e. a decrease of the driving force for cation insertion into the intact and yet cation-free interface. Hence, Fig. 11 instructively shows that the first step has to be the ingress of cations driven by the difference in electrochemical potentials of the cations in the defect and in the coating/metal interface. Only if sufficient cations enter the interface, the decrease in potential is sufficient for initiating sufficient ORR rates causing then delamination. Then the potential is pulled down towards the value in the defect. Otherwise, only migration occurs and the potential will usually remain much higher than the one in the defect.

Finally, the question remains why the rate of cation insertion at the front, which is proposed here to be the rate determining step for both cation migration, if no delamination occurs, and delamination, if sufficient ORR is enabled at the interface, is depending in Tafel like way on the potential difference across the front. In fact, originally this kind of plot – using the potential at the front- was used to check whether an electrochemical reaction such as ORR would be the rate determining step. Then such a Tafel plot like behavior was to be expected. However, the dependence of the rates on cation size speaks against ORR as the rate determining step, as well as the curves for quite high potential at the front where no delamination is observed (see Fig. 6 where upon switch to the highest potential the potential at the migrated interface does not follow or follows only very slowly, as discussed above). Hence, ORR does not play a role for the progress. Now the question is whether the insertion of the cations at the front has to be considered as an electrochemical process, which would fit to the dependence of the logarithm of rate on the potential difference across the front. This is the object of current research.

One interesting point shall be pointed out here: A common assumption is that for a very delamination resisting coating or coating system, e.g. with a phosphate layer, it is the high inhibition of ORR that results in the high suppression of cathodic delamination. However, if this were the case, the progress of cation migration along the interface should still be detectable by SKP. It just would not result in delamination. However, to the best of our knowledge such a migration of cations, leading to a limited pull-down of potential and progress of an according front of change in potential was never observed on slowly delaminating coatings. This in turn means that on such strong coatings the cation migration has also to be inhibited, even more than the ORR. This would make it again most likely the rate determining process of delamination. Whether for very strong coatings also ORR could be rate determining is object of current research. It is pointed out here that it is unclear whether that inhibition of cation incorporation at the interface is rather thermodynamical or kinetical in nature. From the thermodynamic point of view Eqs. (4) and (5) imply that there is always some ingress of cations into the intact interface expected, as long as the cation concentration at the interface is still extremely low. However, how low it has to be that a driving force for cation uptake into the interface exists, depends on the difference of the standard chemical potentials of the cations in the electrolyte and at the intact unaffected interface and also on the

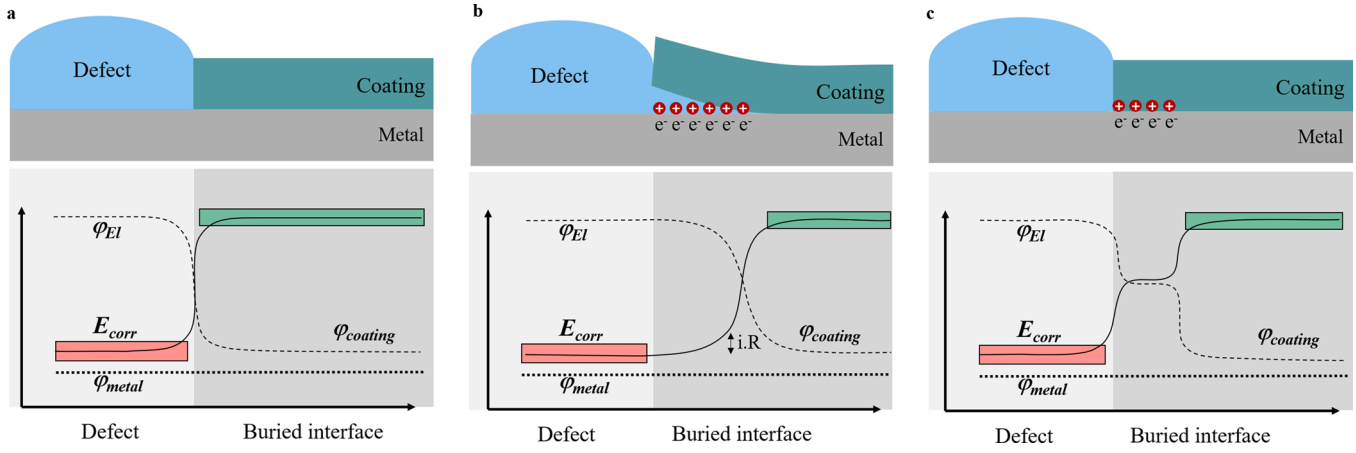

Fig. 12. Sketch of the relative position of the Galvani potentials in the metal and in the phase above it (electrolyte in the defect site, thin water/gel film or organic coating in the delaminating or intact area) and the corresponding electrode potential in case of a) starting situation: corrosion in a defect and intact interface, b) coating delamination (highly concentrated electrolyte in the defect), and c) cation insertion/migration along the interface (dilute electrolyte in the defect), for the case of not sufficiently low potential caused by this insertion for resulting in delamination. In case that the interface is not delaminated, the pull down of potential is determined by the concentration of cations entering the interface and the capacity of that interface (note that the cations are accompanied by electrons in the metal directly at the interface). If the potential is pulled down low enough to result in sufficient oxygen reduction to result in delamination, then as a consequence of delamination it will be pulled down towards the potential of the defect, due to the galvanic coupling with it, only different by the according iR drop.

difference in the Galvani potentials in the two phases. It is possible that for a very delamination resistive coating the necessary concentration is so low that it is already reached by residual contamination at the interface. Then cation ingress into the interface would be thermodynamically unfavored. It is also possible that just the mobility of the cations is significantly reduced, so that the ingress is hindered due to this low mobility. This needs to be further investigated. For not very resistive coatings, on the other hand, if the potential in the defect is low and the concentration of cations is high enough, this cation ingress will pull down the potential at the interface to such extent that ORR can occur and leads to delamination. The progress is, however, still determined by the cation insertion at the front.

The new hypothesis proposed here is schematically summed up in Fig. 12.

4. Conclusion

Fundamental research was conducted on PVB coated iron using a combined SKP/potentiostat set-up in order to elucidate the underlying key parameters of cathodic delamination. The established knowledge thus far was that a square root dependence of delamination on time is associated with cation migration from the defect along the delaminated interface, and a linear dependence on time is attributed to the oxygen reduction reaction as rate determining steps. However, the results presented here show that cation migration along the delaminated interface is rather fast, and therefore, it is unlikely to be a rate determining step in delamination. For the samples studied here, based on our results oxygen reduction reaction as a rate determining step can also be ruled out, due to the dependence of kinetics on cation size and the inhibition of ORR at high potentials, where still a linear progress of front was observed for the occurring cation migration.

Furthermore, the effect of ohmic potential drop in the delaminated interface on delamination rate was studied using potential controlled defects. It was found out that the progress of the front approached a linear dependence on time by decreasing i.R drop at higher applied potentials in the defect. The results also showed that the delamination rate is different for different cations with the same electrochemical driving force for delamination/migration. Based on the results, a new hypothesis about the rate determining step in cathodic delamination is proposed, which is defined as cation insertion. It is suggested that the first insertion of cations into the cation-free intact interface is the rate determining step in delamination, which is in accordance with the obtained results. This new hypothesis also makes it possible to link the delamination resistance to the pore structure and resistance for ionic mobility of the coating/metal interface at the front, which makes more sense than the old migration theory, suggesting cation migration in the delaminated region controls the kinetics. Corrosion driven delamination experiments with dilute solutions in the defect also confirmed the new theory, indicating the first step has to be the ingress of cations driven by the electrochemical potential gradient. Regardless of whether the rate of the progress of delamination/migration is constant with time or depends on the square root of time, the controlling step can still be the same. For the samples investigated here, the parabolic dependence is just the effect of decreasing potential difference across the front, caused by the overall increasing iR drop along the interface. In this context there might be coatings where the dependence on this potential difference, envisioned as the driving force for cation insertion, is very high, which would lead to a parabolic behavior for even relatively low iR drops.

We propose that for relatively weak coatings, this cation insertion step is always the rate determining step. Its importance for delamination resistant coatings is object of current research. It is, however, pointed out here that in any case the decrease of potential at the delamination front is a prerequisite for oxygen reduction and subsequent delamination. And this decrease of potential always first requires the ingress of cations. Finally, it is pointed out that a sharp delamination front in SKP measurements is indicative for cation insertion as rate determining step. If ORR was rate determining, then some cation insertion and migration should advance the delamination, which should lead to a smeared out front.

CRediT authorship contribution statement

Negar Khayatan: Conceptualization, Methodology, Formal analysis, Investigation, Writing – original draft, Writing – review & editing. **Michael Rohwerder**: Conceptualization, Methodology, Funding acquisition, Supervision, Writing – review & editing.

Declaration of Competing Interest

The authors declare that they have no known competing financial interests or personal relationships that could have appeared to influence the work reported in this paper.

Data Availability

The raw/processed data required to reproduce these findings cannot be shared at this time due to legal or ethical reasons.

Acknowledgements

The authors acknowledge “The Research Foundation – Flanders (Fonds Wetenschappelijk Onderzoek – Vlaanderen (FWO), Belgium)” for financial supports. This work is a part of the SBO project PredictCor (project number: FWOSBO22), coordinated by Prof. H. Terryn, Vrije Universiteit Brussel.

References

[1] E. Bardal, Corrosion and Protection, Springer, London, 2004.
[2] O.Ø. Knudsen, A. Forsgren, Corrosion Control through Organic Coatings, CRC Press, 2017.
[3] H. Leidheiser Jr., W. Wang, L. Igetoft, The mechanism for the cathodic delamination of organic coatings from a metal surface, Prog. Org. Coat. 11 (1983) 19–40.
[4] W. Fürbeth, M. Stratmann, Investigation of the delamination of polymer films from galvanized steel with the Scanning Kelvinprobe, Fresenius J. Anal. Chem. 353 (1995) 337–341.
[5] M. Stratmann, The investigation of the corrosion properties of metals, covered with adsorbed electrolyte layers—a new experimental technique, Corros. Sci. 27 (1987) 869–872.
[6] M. Stratmann, R. Feser, A. Leng, Corrosion protection by organic films, Electrochim. Acta 39 (1994) 1207–1214.
[7] M. Stratmann, A. Leng, W. Fürbeth, H. Streckel, H. Gehmecker, K.-H. Große-Brinkhaus, The scanning Kelvin probe; a new technique for the in situ analysis of the delamination of organic coatings, Prog. Org. Coat. 27 (1996) 261–267.
[8] M. Stratmann, H. Streckel, On the atmospheric corrosion of metals which are covered with thin electrolyte layers—I. Verification of the experimental technique, Corros. Sci. 30 (1990) 681–696.
[9] M. Stratmann, H. Streckel, On the atmospheric corrosion of metals which are covered with thin electrolyte layers—II. Experimental results, Corros. Sci. 30 (1990) 697–714.
[10] M. Stratmann, H. Streckel, R. Feser, A new technique able to measure directly the delamination of organic polymer films, Corros. Sci. 32 (1991) 467–470.
[11] M. Stratmann, M. Wolpers, H. Streckel, R. Feser, Use of a scanning-kelvinprobe in the investigation of electrochemical reactions at the metal/polymer interface, Ber. Bunsenges.Phys. Chem. 95 (1991) 1365–1375.
[12] S. Yee, R. Oriani, M. Stratmann, Application of a Kelvin microprobe to the corrosion of metals in humid atmospheres, J. Electrochem. Soc. 138 (1991) 55.
[13] A. Leng, H. Streckel, M. Stratmann, The delamination of polymeric coatings from steel. Part 1: Calibration of the Kelvinprobe and basic delamination mechanism, Corros. Sci. 41 (1998) 547–578.
[14] A. Leng, H. Streckel, M. Stratmann, The delamination of polymeric coatings from steel. Part 2: First stage of delamination, effect of type and concentration of cations on delamination, chemical analysis of the interface, Corros. Sci. 41 (1998) 579–597.
[15] A. Leng, H. Streckel, K. Hofmann, M. Stratmann, The delamination of polymeric coatings from steel Part 3: Effect of the oxygen partial pressure on the delamination reaction and current distribution at the metal/polymer interface, Corros. Sci. 41 (1998) 599–620.
[16] R. Krieg, M. Rohwerder, S. Evers, B. Schuhmacher, J. Schauer-Pass, Cathodic self-healing at cut-edges: the effect of Zn2+ and Mg2+ ions, Corros. Sci. 65 (2012) 119–127.

[17] R. Hausbrand, M. Stratmann, M. Rohwerder, The physical meaning of electrode potentials at metal surfaces and polymer/metal interfaces: consequences for delamination, J. Electrochem. Soc. 155 (2008) C369.
[18] M. Rohwerder, Passivity of metals and the kelvin probe technique, in: reference module in chemistry, molecular sciences and chemical engineering, encyclopedia of interfacial chemistry. Surface Science and Electrochemistry, Elsevier, 2018, pp. 414–422.
[19] W. Fürbeth, M. Stratmann, The delamination of polymeric coatings from electrogalvanized steel–a mechanistic approach.: Part 3: delamination kinetics and influence of CO_2, Corros. Sci. 43 (2001) 243–254.
[20] J. Sharman, J. Sykes, T. Handyside, Cathodic disbonding of chlorinated rubber coatings from steel, Corros. Sci. 35 (1993) 1375–1383.
[21] G. Williams, H. McMurray, Chromate inhibition of corrosion-driven organic coating delamination studied using a scanning Kelvin probe technique, J. Electrochem. Soc. 148 (2001) B377.
[22] G. Williams, H. McMurray, D. Worsley, Cerium (III) inhibition of corrosion-driven organic coating delamination studied using a scanning Kelvin probe technique, J. Electrochem. Soc. 149 (2002) B154.
[23] M. Hernandez, F. Galliano, D. Landolt, Mechanism of cathodic delamination control of zinc–aluminum phosphate pigment in waterborne coatings, Corros. Sci. 46 (2004) 2281–2300.
[24] R. Holness, G. Williams, D. Worsley, H. McMurray, Polyaniline inhibition of corrosion-driven organic coating cathodic delamination on iron, J. Electrochem. Soc. 152 (2005) B73.
[25] P.A. Sørensen, K. Dam-Johansen, C.E. Weinell, S. Kiil, Cathodic delamination: quantification of ionic transport rates along coating–steel interfaces, Prog. Org. Coat. 68 (2010) 70–78.
[26] D.J. Warren, H.N. McMurray, A.C. de Vooys, Localised SKP studies of cathodic disbondment on chromium/chromium oxide coated steel, ECS Trans. 50 (2013) 67.
[27] N. Wint, S. Geary, H. McMurray, G. Williams, A. de Vooys, The kinetics and mechanism of atmospheric corrosion occurring on tin and iron-tin intermetallic coated steels, J. Electrochem. Soc. 162 (2015) C775.
[28] H. Bi, J. Sykes, Cathodic delamination of unpigmented and pigmented epoxy coatings from mild steel, Prog. Org. Coat. 90 (2016) 114–125.
[29] C. Glover, C. Richards, G. Williams, H. McMurray, Evaluation of multi-layered graphene nano-platelet composite coatings for corrosion control part II–Cathodic delamination kinetics, Corros. Sci. 136 (2018) 304–310.
[30] A. Nazarov, N. Le Bozec, D. Thierry, Assessment of steel corrosion and deadhesion of epoxy barrier paint by scanning Kelvin probe, Prog. Org. Coat. 114 (2018) 123–134.
[31] J.E. Edy, H.N. McMurray, K.R. Lammers, C. Arnoud, Kinetics of corrosion-driven cathodic disbondment on organic coated trivalent chromium metal-oxide-carbide coatings on steel, Corros. Sci. 157 (2019) 51–61.
[32] G. Williams, C. Kousis, N. McMurray, P. Keil, A mechanistic investigation of corrosion-driven organic coating failure on magnesium and its alloys, npj Mater. Degrad. 3 (2019) 1–8.
[33] J.M. Prabhakar, R.S. Varanasi, C.C. da Silva, A. de Vooys, A. Erbe, M. Rohwerder, Chromium coatings from trivalent chromium plating baths: characterization and cathodic delamination behaviour, Corros. Sci. 187 (2021), 109525.
[34] A. Merz, M. Uebel, M. Rohwerder, The protection zone: a long-range corrosion protection mechanism around conducting polymer particles in composite coatings: Part I. polyaniline and polypyrrole, J. Electrochem. Soc. 166 (2019) C304.
[35] A. Merz, M. Rohwerder, The protection zone: a long-range corrosion protection mechanism around conducting polymer particles in composite coatings: part II. PEDOT: PSS, J. Electrochem. Soc. 166 (2019) C314–C320.
[36] M. Uebel, A. Vimalanandan, A. Laaboudi, S. Evers, M. Stratmann, D. Diesing, M. Rohwerder, Fabrication of robust reference tips and reference electrodes for Kelvin probe applications in changing atmospheres, Langmuir 33 (2017) 10807–10817.
[37] M. Uebel, Release and transport of corrosion inhibitors in self-healing coatings for intelligent corrosion protection, Ruhr Univ. Boch. (2019), https://doi.org/10.13154/294-6477.
[38] A.W. Hassel, K. Fushimi, M. Seo, An agar-based silver| silver chloride reference electrode for use in micro-electrochemistry, Electrochem. Commun. 1 (1999) 180–183.
[39] V. Shkirskiy, M. Uebel, A. Maltseva, G. Lefèvre, P. Volovitch, M. Rohwerder, Cathodic driven coating delamination suppressed by inhibition of cation migration along Zn| polymer interface in atmospheric CO 2, npj Mater. Degrad. 3 (2019) 1–10.
[40] K. Wapner, M. Stratmann, G. Grundmeier, In situ infrared spectroscopic and scanning Kelvin probe measurements of water and ion transport at polymer/metal interfaces, Electrochim. Acta 51 (2006) 3303–3315.